



CHORUS

This is the accepted manuscript made available via CHORUS. The article has been published as:

Experimental evidence for the microscopic mechanism of the unusual spin-induced electric polarization in $\text{GdMn}_{2}\text{O}_{5}$

G. Yahia, F. Damay, S. Chattopadhyay, V. Balédent, W. Peng, S. W. Kim, M. Greenblatt, M.-B. Lepeitit, and P. Foury-Leylekian

Phys. Rev. B **97**, 085128 — Published 15 February 2018

DOI: [10.1103/PhysRevB.97.085128](https://doi.org/10.1103/PhysRevB.97.085128)

Experimental evidences of the microscopic mechanism for the unusual spin-induced electric polarization in GdMn_2O_5

G. Yahia,^{1,2} F. Damay,³ S. Chattopadhyay*,^{4,5} V. Balédent,¹ W. Peng,¹
S. W. Kim,⁶ M. Greenblatt,⁶ M.-B. Lepetit,^{7,8} and P. Foury-Leylekian¹

¹*Laboratoire de Physique des Solides, CNRS, Univ. Paris-Sud, Université Paris-Saclay 91405 Orsay cedex, France*

²*Laboratoire de Physique de la Matière Condensée, Université Tunis-El Manar, 2092 Tunis, Tunisia*

³*Laboratoire Léon Brillouin, CEA-CNRS UMR12 91191 Gif-sur-Yvette Cedex, France*

⁴*Université Grenoble Alpes, INAC-MEM, F-38000 Grenoble, France*

⁵*CEA-Grenoble, INAC-MEM, F-38000 Grenoble, France*

⁶*Department of Chemistry and Chemical Biology, Rutgers, the State University of New Jersey, Piscataway, NJ 08854 USA*

⁷*Institut Néel, CNRS UPR 2940, 25 av. des Martyrs, 38042 Grenoble, France*

⁸*Institut Laue Langevin, 72 av. des Martyrs, 38042 Grenoble France*

We report in this paper the temperature evolution of the magnetic structure of GdMn_2O_5 , in the range 2 K to 40 K, studied by neutron diffraction on an isotope enriched powder. We detail a thorough analysis of the the microscopic mechanisms needed to release the different magnetic frustrations that are at the origin of the polarization. In addition to the usual exchange-striction term, known to be at the origin of the polarization in this family, an additional exchange-striction effect between the Gd^{3+} and Mn^{3+} spins is found to be responsible for the very large polarization in the Gd compound.

Multiferroic materials, stabilizing at least two different but simultaneous orders, generally magnetism and ferroelectricity, are potentially useful materials for applications, owing to their versatility and multi-functionality [1]. For the technological development of magneto-electric multiferroics, the optimization of performances such as the coupling between magnetic and ferroelectric orders is required. This optimization is, however, challenging, since most of the current magneto-electric multiferroic materials present either a weak electric polarization or a weak magneto-electric coupling.

Recently, a sizable magneto-electric effect has been measured in several members of the RMn_2O_5 (R= rare earth) manganites [2]. GdMn_2O_5 , for instance, presents an electric polarization of $\sim 3600 \mu\text{C}/\text{m}^2$ [3–5], a value nearly able to compete with the so-called Bi manganite multiferroics [6]. In addition, its unusually strong electric polarization is also highly sensitive to applied magnetic fields [3]. The challenge is to understand the microscopic origin of this spin induced ferroelectricity, and to pinpoint the specificity of Gd among other rare-earths. In most of the spin induced multiferroics, the Dzyaloshinskii-Moriya interaction between non colinear spins has been proposed as the microscopic mechanism of the magnetic ferroelectricity. However in the case of the RMn_2O_5 family, the observation of a perfectly colinear spin arrangement along the c axis in SmMn_2O_5 , has recently definitively ascribed the ferroelectricity to an Mn-Mn exchange-striction model [7]. Gd-Mn symmetric exchange striction, in addition to the Mn-Mn exchange striction mechanism, have recently been suggested in order to explain the large polarization measured in GdMn_2O_5 [3] but without any proposed microscopic mechanism. Moreover, the determination of the GdMn_2O_5 magnetic structure was done using resonant

X-ray magnetic scattering which provides no information on the moments' absolute value or their relative phases.

For a more accurate understanding of the origin of the unusually large polarization of GdMn_2O_5 a precise magnetic structure determination is required, ideally from neutron scattering experiments. Owing to the extremely high neutron absorption of the Gd nucleus, such an experiment had never been attempted to date. We present in this paper the first powder neutron diffraction experiment performed on an isotope (^{160}Gd) enriched compound. From this measurement we deduce the magnetic structure as a function of the temperature. Furthermore, by a detailed analysis of the exchange terms, we show evidence of the microscopic mechanism responsible for the strong electric polarisation in the Gd member.

The RMn_2O_5 compounds crystallize in the Pm space group [8]. Nevertheless, owing to the small distortions away from the average $Pbam$ structure, the latter will be used in the magnetic refinements which will follow. Along the c direction, the RMn_2O_5 structure is composed of chains of Mn^{4+}O_6 octahedra, separated by layers of R^{3+} or Mn^{3+} ions. In the (a, b) plane, zig-zag chains of Mn^{4+}O_6 octahedra and Mn^{3+}O_4 pyramids run along the a axis, and are stacked along the b axis (see Figure 1).

Along c , there are two relevant $\text{Mn}^{4+} - \text{Mn}^{4+}$ exchange interactions, J_1 (through the R^{3+} layers) and J_2 (through the Mn^{3+} layers) [9]. While J_2 is intrinsically antiferromagnetic, it is strongly frustrated by the $\text{Mn}^{4+} - \text{Mn}^{3+}$ interactions. This always results in a ferromagnetic ordering of the Mn^{4+} ions. The case of the J_1 interaction is more complex and leads to the various incommensurate magnetic orders observed in the RMn_2O_5 members when R is varied. The magnetic frustration inherent to this structure comes mostly from the exchange interactions in the (a, b) plane. There are three non equivalent

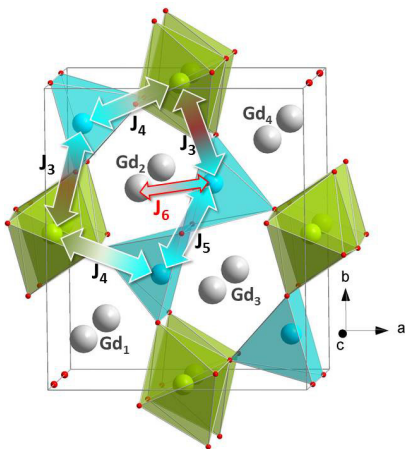


FIG. 1: (Color online) Perspective view of the RMn_2O_5 crystal structure and relevant magnetic exchanges. The Mn^{4+} (green) ions are in an octahedral coordination shell and the Mn^{3+} (cyan) ions are in a square-based pyramidal coordination shell. Exchange terms J_i are detailed in the text.

magnetic super-exchange paths, J_3 and J_4 between Mn^{4+} and Mn^{3+} spins, and J_5 between two Mn^{3+} spins (Figure 1). The main contribution to these exchanges is the antiferromagnetic (AF) Mn-Mn super-exchange interaction through a shared oxygen. J_4 and J_5 are expected to be the dominant integrals [10], while J_3 is frustrated. The influence of the rare earth is generally neglected in the exchange Hamiltonian, owing to the strong spatial localization of their orbitals. However at low temperature and in the particular case of Gd^{3+} with its giant spin ($4f^7$ electronic configuration), the super-exchange interaction between $\text{Gd}^{3+} - \text{Mn}^{3+}$ spins through a common oxygen (labeled J_6 in the following and on Figure 1) can become relevant as first proposed in reference [11]. The fingerprint of the importance of this J_6 interaction has recently been identified using inelastic neutron scattering in DyMn_2O_5 [12]. Notice that another exchange interaction between Mn^{4+} and R^{3+} has been introduced by Zhao et al [13] but is expected to be smaller than the one involving Mn^{3+} , and can be shown to be irrelevant for the onset of the polarization.

Previous heat capacity measurements performed on GdMn_2O_5 have evidenced a succession of three phase transitions, at $T_1 \simeq 38$ K, $T_2 \simeq 32$ K and $T_3 \simeq 5$ K [14]. The low temperature transition is not accurately defined because of the width of the heat capacity peak, which spreads from 10 K to 2 K. Concomitantly with the T_2 transition, a sharp peak is observed in the real part of the dielectric constant, with a shoulder already present at T_1 [5]. Below a temperature close to T_3 , another peak is observed in the dielectric constant measurement [15]. Furthermore, polarization measurements show that between T_1 and T_2 , the b component of the polarization

is minute and starts to really develop only below T_2 . It slightly increases below 10 K but does not saturate down to 2 K.

The measurements presented in this paper were performed on a high purity and high quality powder, whose synthesis was carried out following the process described in reference [16], starting from a ^{160}Gd enriched Gd_2O_3 oxide.

Neutron powder diffraction experiments were carried out on a 1g powder sample, on the G4.1 diffractometer (Orphée-LLB, CEA-Saclay, France). The neutron wavelength was 2.426 Å. Measurements were performed by heating up the sample from 2 K to 40 K, with a step of 4 K above 4 K. Rietveld refinements of the crystal and magnetic structures were performed with the FULLPROF program [17], and symmetry analysis was performed using tools from the Bilbao crystallographic server (see reference [18] and references within).

The temperature evolution of the diffractograms is shown on Figure 2. The results evidence three magnetic transitions at $T_1 = 40$ K, $T_2 = 32$ K and $T_a = 12$ K. T_1 and T_2 coincide with the presence of the anomalies in the heat capacity and dielectric constant measurements, while at T_a , an anomaly in the temperature dependence of the electric polarization has been detected by various authors [3, 19, 20].

The propagation wave vector between T_1 and T_2 is of the type $\mathbf{q}_{\text{ICM}} = (0.5 - \delta_1, 0, 0.2 - \delta_2)$, compatible with the reported $(0.49, 0, 0.18)$ [3]. Only two very weak and broad magnetic Bragg peaks can be seen on the 36 K diffraction pattern (see bottom panel of Figure 2), thus preventing any accurate description of the magnetic ordering in this temperature range. Below T_2 , in contrast, several new magnetic Bragg reflections appear (Figure 2). These reflections can be indexed with a commensurate magnetic propagation vector $\mathbf{q}_{\text{CM}} = (0.5, 0, 0)$. The magnetic intensity at low temperature is much stronger than generally observed in the other compounds of the series, indicating a strong magnetic contribution of the Gd^{3+} spins.

As the symmetry breaking from the $Pbam$ to Pm space groups remains weak in the RMn_2O_5 family, the symmetry analysis was performed starting from the $Pbam\bar{1}$ paramagnetic group. There are four possible maximal subgroups compatible with a \mathbf{q}_{CM} magnetic ordering. As reported [3], only $P_a ca 2_1$ (or $P_a b 2_1 a$ in the parent cell setting) provides a satisfactory refinement of the diffraction data. Note that it is also the only allowing a collinear arrangement of the Gd and Mn species spins, and a non-zero polarization tensor along b . In this magnetic space group, because of the loss of inversion symmetry, there are two pairs of Gd ((Gd1, Gd2) and (Gd3, Gd4), Fig. 1), which are independent. Within each pair, Gd spins are related by a 2_1 or a $2'_1$ rotation. There are two distinct Mn^{3+} pairs as well. In order to reduce the number of free parameters in the refinement, the magnitude of the moments for same species ions were initially set to be equal.

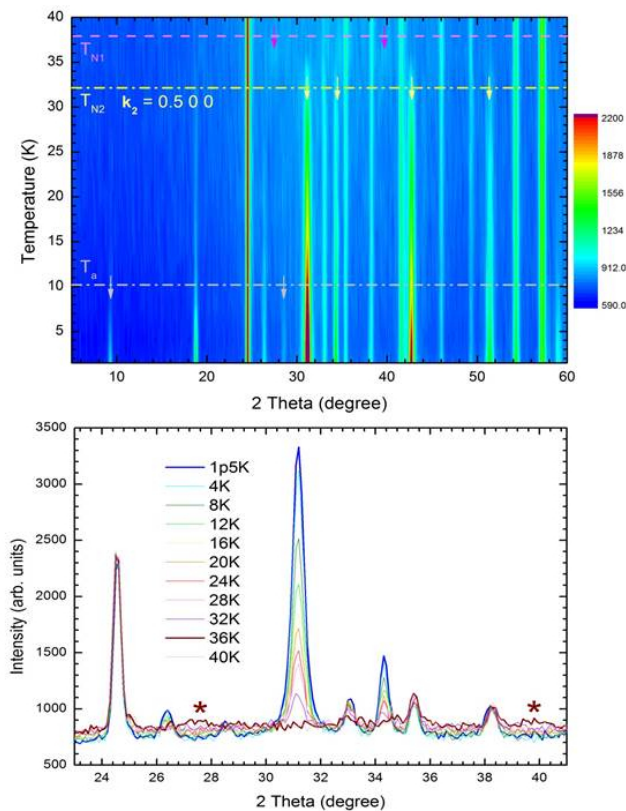


FIG. 2: (color online) Temperature evolution of the powder neutron diffraction patterns of GdMn_2O_5 between 40 and 2 K. The bottom panel is a zoom on the main magnetic Bragg peak profile in the same temperature range. Stars correspond to the two magnetic peaks identified at 36 K in the incommensurate magnetic phase.

Releasing the constraint on the Gd^{3+} moments amplitudes however leads to a substantial improvement of the refinement. The best Rietveld profile at 1.5 K is shown on Figure 3, and the corresponding magnetic order on Figure 4.

The results of the refinement show that at 1.5 K, all the moments lie in the (a, b) plane, with a systematically larger component along a than along b (see also Table I). The usual feature of TbMn_2O_5 , that is, the antiferromagnetic ordering (due to J_5) between edge-sharing Mn^{3+} tetrahedra pairs (blue ellipse on Figure 4), is also found in GdMn_2O_5 . The antiparallel arrangement of specific Gd/Mn^{3+} pairs (orange ellipse on Figure 4) is also striking, as it is not an imposed constraint. Mn^{4+} spins lie within the equatorial plane of their octahedral environment. The Gd moments are nearly fully ordered, between $5.5 \mu_B$ for the (Gd1, Gd2) pair and $6.4 \mu_B$ for the (Gd3, Gd4) pair, at 1.5 K. Mn^{3+} and Mn^{4+} moment values are comparable to those published for other members of the RMn_2O_5 series, with 3.3 and $2.6 \mu_B$, respectively, at

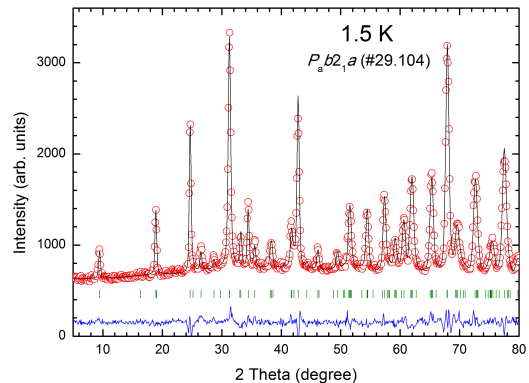


FIG. 3: (color online) Rietveld refinement of the neutron diffraction data of GdMn_2O_5 at 1.5 K. The experimental data are in red, the calculated profile in black, and their difference in blue. Green ticks indicate Bragg peaks positions.

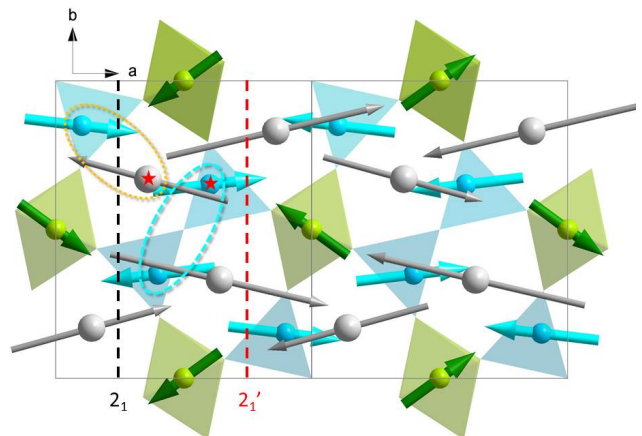


FIG. 4: (color online) Magnetic structure of GdMn_2O_5 at 1.5 K. The blue (orange) ellipses show the $\text{Mn}^{3+}/\text{Mn}^{3+}$ ($\text{Gd}^{3+}/\text{Mn}^{3+}$) AF pairs. Stars identify the Gd/Mn^{3+} pair proposed by Lee et al. in their model [3].

1.5 K. Note that the magnetic ordering proposed by Lee et al. [3] is almost in perfect agreement with the one determined here from neutron diffraction. The main difference is in the Gd/Mn antiparallel pairs, which couple in the X-ray model the closest Mn-Gd atoms (outlined by stars on Figure 4). Another minor difference lies in the estimation of the ordered moment, which is in this study slightly higher for Gd and lower for Mn spins, as Lee et al. had to assume that Mn spins were saturated at their spin-only expected value, which is not quite the case, according to our results.

It is possible, with increasing temperature, to use the

TABLE I: (color online) Magnetic structure parameters of GdMn_2O_5 at 1.5 K in the $P_a b 2_1 a$ cell (i.e., doubled along a).

	x/a	y/b	z/c	M_x	M_y	$M_{tot}(\mu_B)$
Mn^{3+}	0.199	0.348	0.5	-3.3(1)	-0.4(1)	3.3(1)
Mn^{4+}	0	0.5	0.252	2.2(1)	-1.4(1)	2.6(1)
Gd1	0.07	0.169	0	5.4(1)	0.9(1)	5.5(1)
Gd3	0.923	0.831	0	-6.3(1)	-1.3(1)	6.4(1)

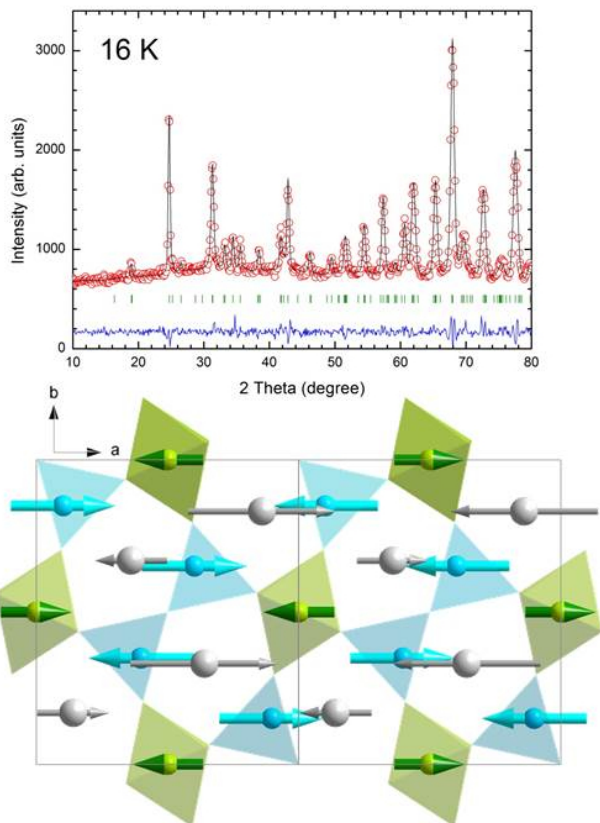


FIG. 5: (color online) Rietveld refinement and corresponding magnetic structure of GdMn_2O_5 at 16 K.

same model to refine the diffraction data. However, above 12 K, the disappearance of two reflections, namely (100) and (300), allows one to propose a model of the magnetic structure where all spins are aligned along a , without deteriorating the refinement (see Figure 5). Although this is not a definite proof that the magnetic structure is actually collinear, it would explain the anomaly seen around 12K, as the temperature at which spins depart from collinearity. The evolution of the ordered moment with temperature is shown on Figure 6, and does not depend (within the error bars) on the model chosen to refine the data. Two interesting conclusions can be made from this evolution : first, that Gd moments order

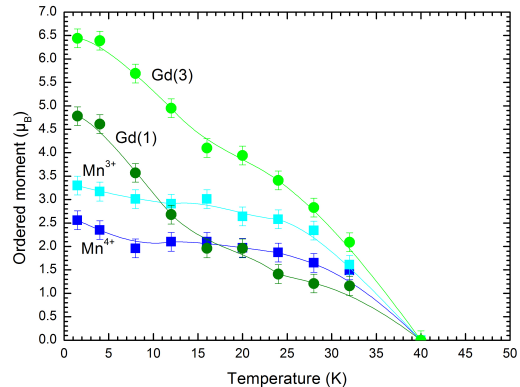


FIG. 6: (color online) Temperature evolution of the magnetic moments on the Mn^{4+} , Mn^{3+} and Gd^{3+} sites in GdMn_2O_5 (from Rietveld refinements of neutron diffraction data, assuming a collinear magnetic structure above 16 K).

as early as 32 K, as was already intuited by several authors [3], and second, from the shape of the Gd moment vs. T curve, that Gd moments do order in the effective magnetic field created by the Mn spins ordering. We applied the molecular-field model in order to calculate these thermal variations. The temperature dependence of the Mn mean moments is determined by the usual self-consistent mean-field calculation [21], giving a coupling $\lambda_0 = 10.6 \pm 0.6 T \mu_B^{-1}$. A similar fit for the mean moments of the two Gd in the molecular field of the mean Mn moments gives a coupling value of $\lambda_1 = 2.4 \pm 0.1 T \mu_B^{-1}$ (see Fig. 7). The coupling between Gd and Mn is then 4 times smaller than that of the coupling between Mn and Mn. The main contributions to Mn-Mn coupling come from J_4 and J_5 ($\approx 2.9\text{meV}$ and 3.5meV in TbMn_2O_5 [10]) since J_1 and J_2 are an order of magnitude smaller ($\approx 0.4\text{meV}$ in TbMn_2O_5 [10]) and J_3 fully compensated within the $Pbam$ mean space group and thus not contributing. We can then expect the coupling between Mn and Gd (related to an effective J_6) to be one fourth of J_4 and J_5 , and thus around 0.7meV .

At this point let us redo the magnetic symmetry analysis from a quantum mechanical point of view. One should first remember that in quantum mechanics the symmetry of a system is not related to the space-time operators leaving its ground-state (or its magnetic part) invariant (as assumed in magnetic diffraction), but that the magnetic space-group is the set of space-time symmetry operators leaving the hamiltonian of the system invariant. In the Born-Oppenheimer approximation (fixed, classical nuclei), it means the set of operators leaving the electrostatic potential generated by the nuclei and the spin-orbit operators invariant. Group theory then tells us that the ground-state wave-function, Ψ , and thus its magnetic

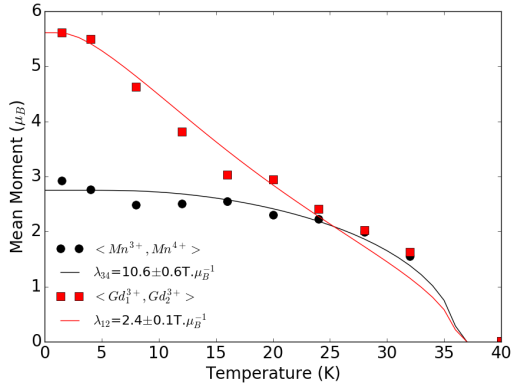


FIG. 7: Temperature dependence of mean Mn (black circles) and Gd (red squares) moments. Lines correspond to the self-consistent mean-field calculation fit for Mn and Gd in the molecular field of the mean Mn moments.

part, must belong to one of the irreducible corepresentations, Γ_n , of the magnetic group \mathcal{G} , but not necessarily to the totally symmetric Γ_1 one. In other words one must have: $\forall \hat{g} \in \mathcal{G}, \hat{g}\Psi = \lambda_g \Psi$ with $\lambda_g \in \mathbb{C}$, but not necessarily $\forall \hat{g} \in \mathcal{G}, \lambda_g = 1$ characteristic of the Γ_1 irreducible representation. Diffraction data tells us that the crystallographic group for the RMn_2O_5 family is Pm [8]. It is easy to show that the magnetic group is $\mathcal{G}: Pm'$ (see supplementary material). At the X point $(1/2\ 0\ 0)$ of the Brillouin zone, the Pm' group has two irreducible corepresentations, X_1 and X_2 . According to group theory, states belonging to X_1 are symmetric with respect to m' , while states belonging to X_2 are asymmetric. Applied to the magnetic moments of the Mn and Gd ions it means that

within X_1 : each of the Gd^{3+} , Mn^{3+} and Mn^{4+} within the unit cell are independant, the Gd^{3+} and Mn^{3+} moments must be in the (a, b) plane, while there are no conditions on the orientation of the Mn^{4+} moments ;

within X_2 : each of the Gd^{3+} , Mn^{3+} and Mn^{4+} within the unit cell are independant, the Gd^{3+} and Mn^{3+} moments must be along c , while there are no conditions on the orientation of the Mn^{4+} moments.

One sees immediately that the magnetic structure found for the GdMn_2O_5 compound thus belongs to the X_1 irreducible representation of the magnetic Pm' group.

In the framework of the exchange-striction mechanism (ES), we can precisely describe the mechanism at the origin of the electric polarization created by the magnetic order in GdMn_2O_5 and more generally in the RMn_2O_5 compounds. Let us recall that the magnetic frustration within the Mn pentagons is directly related to the J_3 magnetic exchanges (Figure 1). Indeed, in the $Pbam$

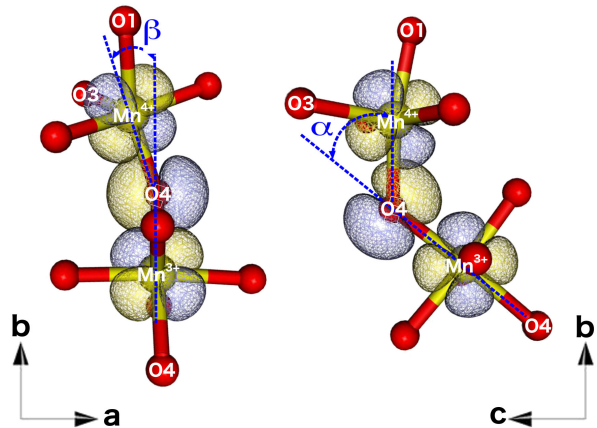


FIG. 8: (color online) Super-exchange paths for the J_3 magnetic exchange (see Fig. 1) in the (a, b) and (b, c) planes. With this angle convention,

$$J_3 \simeq J_{\pi\pi} \cos \beta + J_{\pi\pi} \cos \alpha$$

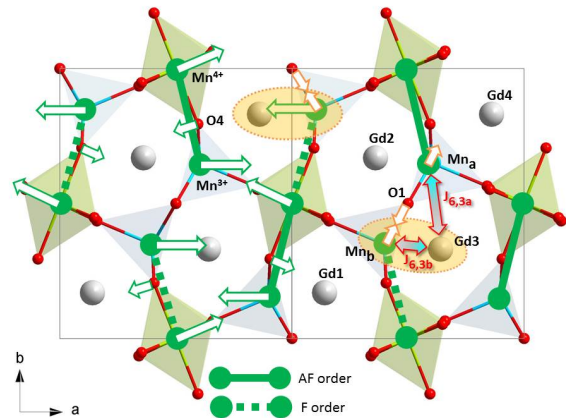


FIG. 9: (color online) Atomic displacements associated with the release the magnetic frustration at the origin of the polarization. On the left half of the unit cell, displacements represented by green arrows are due to the Exchange-Striction mechanism involving J_3 (Fig. 8). On the right half, gold arrows stand for displacements due to the additional Exchange-Striction mechanism involving J_6 . Gold ellipses englobe the $Gd-Mn^{3+}$ coupled by J_6 via O_1 . The global displacement is along $+b$ direction for Mn ions and along $(-b)$ for O resulting in a polarization along b .

non-polar group, J_3 does not contribute to the magnetic energy as its two contributions cancel out: in each unit cell one is located between atoms with a FM ordering, while the other is between atoms with an AFM ordering (see Figures 4 or 5). It is thus the symmetry breaking from $Pbam$ to Pm which allows the two J_3 interactions to be inequivalent, that is responsible for the observed

polarization. Indeed, to release the magnetic frustration, one needs atomic displacements increasing the J_3 super-exchange term between antiferromagnetically ordered moments, and decreasing it between ferromagnetically ordered ones [7]. Following the analysis of reference [10], the main way to modify J_3 is to change the angles α and β in order to maximize the $\text{Mn}^{3+}(\text{t}_{2g})$ - $\text{O}_4(2p)$ - $\text{Mn}^{4+}(\text{t}_{2g})$ orbitals' overlap (see Figure 8). Increasing the AFM character of J_3 thus means decreasing α and β towards 0. As a consequence, the Mn^{3+} ions will shift alternatively along the $\pm a$ direction, the Mn^{4+} along the $\pm a + \varepsilon b$, while the O_4 oxygen bridging the Mn^{3+} and Mn^{4+} ions will move alternatively along a $\pm a - \eta b$ direction (see Figure 9). Within the entire unit cell these shifts result in a global relative displacement of the negative charges along $-b$ and of the positive ones along the $+b$ direction, i.e. in a macroscopic electric polarization along b and a symmetry breaking of the inversion center.

To further understand the unusually high value of the polarization in the specific case of GdMn_2O_5 , let us now analyze on the Gd-Mn interactions. One should first remember that the Gd^{3+} ion is in a $4f^7$, $S = 7/2$, $L = 0$ configuration. As a result, in a first approximation (spherical, atomic), the spin-orbit interaction on the Gd^{3+} ground-state and thus the Gd^{3+} magnetic anisotropy are null. Another consequence is a distance-only dependence of some of the factors involved in J_6 . Using the quasi-degenerate perturbation theory [22] on an effective Hubbard model based on the 4f orbitals of the Gd, the 3d orbitals of the Mn and the 2p orbitals of the bridging oxygens, one can write the Gd-Mn super-exchange terms from the fourth order in the usual way (see for instance 23, 24 and related references)

$$J_6 \simeq - \sum_{2p} \sum_i (t_{f,p})^2 (t_{p,d_i})^2 \left(\frac{2}{(\Delta E_f)^2 U_f} + \frac{2}{(\Delta E_d)^2 U_d} \right) \quad (1)$$

where $t_{f,p}$ is the transfer integral between the set of 4f orbitals of the Gd ion and the 2p orbitals of the bridging oxygen, t_{p,d_i} is the transfer integral between the occupied $3d_i$ orbital of the Mn ion and the bridging oxygen 2p orbital, ΔE_f is the ligand-to-Gd charge transfer energy and ΔE_d the ligand-to-Mn charge transfer energy, finally U_f and U_d are the repulsion integrals of a double occupation in the Gd 4f and Mn 3d shells respectively. Due to the $4f^7$ configuration of the Gd^{3+} ion, the Gd-O factors in J_6 only depend on the Gd-O distance. As a result the strongest J_6 interactions should be the ones bridged by the oxygen closest to the Gd. At low temperature this is the O_1 (Fig.9) oxygen, which also mediates the strongest Mn-Mn interaction J_5 . In fact, as can be seen on Fig. 4 and 9, O_1 mediates the interaction between the Mn^{3+} dimer and two Gd ions, namely Gd_2 and Gd_3 (see Fig. 9), resulting in a strong magnetic frustration. Let us investigate, within the framework of an Heisenberg Hamiltonian in mean-field approximation, whether exchange-striction can induce additional atomic displacements that release this frustration. One can model the

local magnetic energy as

$$E = J_{6,2a} \langle \vec{S}_{\text{Gd}_2} \rangle \cdot \langle \vec{S}_{\text{Mn}_a^{3+}} \rangle + J_{6,2b} \langle \vec{S}_{\text{Gd}_2} \rangle \cdot \langle \vec{S}_{\text{Mn}_b^{3+}} \rangle \\ + J_{6,3a} \langle \vec{S}_{\text{Gd}_3} \rangle \cdot \langle \vec{S}_{\text{Mn}_a^{3+}} \rangle + J_{6,3b} \langle \vec{S}_{\text{Gd}_3} \rangle \cdot \langle \vec{S}_{\text{Mn}_b^{3+}} \rangle$$

In a $Pbam$ structural group, one would have :

$$J = J_{6,2a} = J_{6,3a} = J_{6,2b} = J_{6,3b} \\ \vec{s} = \langle \vec{S}_{\text{Mn}_a^{3+}} \rangle = -\langle \vec{S}_{\text{Mn}_b^{3+}} \rangle \\ \vec{S} = -\langle \vec{S}_{\text{Gd}_2} \rangle = \langle \vec{S}_{\text{Gd}_3} \rangle$$

with $J_{6,ia}$ the exchange term between Gd_i and Mn_a (see Fig. 9), resulting in $E = 0$. In a subgroup compatible with the disproportionation of all the Gd moments as observed in the 1.5 K magnetic structure one has

$$\vec{S}_2 = \langle \vec{S}_{\text{Gd}_2} \rangle \neq \vec{S}_3 = -\langle \vec{S}_{\text{Gd}_3} \rangle \quad \text{and} \quad S_2 < S_3$$

and thus $E = J \left[\vec{S}_2 \cdot (\vec{s} - \vec{s}) + \vec{S}_3 \cdot (\vec{s} - \vec{s}) \right] = 0$. In order to release the magnetic frustration and lower E one therefore needs further action, as for instance atomic displacements. Indeed, a movement increasing the amplitude of the J_6 interaction coupling the largest AFM Gd_3 - Mn_b interaction (as $S(\text{Gd}_3) > S(\text{Gd}_1)$) should lower the magnetic energy, as can be seen in the following equations

$$J_a = J_{6,2a} = J_{6,3a} \neq J_b = J_{6,2b} = J_{6,3b} \quad \text{and} \quad |J_a| < |J_b| \\ \vec{S}_2 = \langle \vec{S}_{\text{Gd}_2} \rangle \neq \vec{S}_3 = -\langle \vec{S}_{\text{Gd}_3} \rangle \quad \text{and} \quad S_2 < S_3$$

that yield

$$E = (J_a - J_b) (\vec{S}_3 - \vec{S}_2) \cdot \vec{s} < 0$$

As can be seen from Eq. 1, such atomic displacements must increase the $(t_{p,d_i})^2$ factors and thus the overlap between the oxygen 2p orbitals and the Mn_b^{3+} 3d ones. Indeed, as the Mn-Gd magnetic exchanges are mediated by the oxygens (see eq. 1), a displacement of the Gd ions will result in an equal modification of $J_{6,2b}$ and $J_{6,3b}$ (similarly $J_{6,2a}$ and $J_{6,3a}$) and thus will not lift the frustration. It means that one must shorten the O_1 - Mn_b^{3+} bond and lengthen the O_1 - Mn_a^{3+} bond, as pictured on the right part of Fig. 9. These displacements do not interfere with the original exchange-striction, issued from the release of the J_3 frustration. They result in a further increase of the polarization along b , responsible for the very large value of the GdMn_2O_5 polarization among the RMn_2O_5 family.

The possibility of an additional mechanism has been previously proposed, but neither experimentally demonstrated nor explicit until now [3, 19].

At 12 K the structural data exhibit a cross over between the Gd- O_1 and Gd- O_2 distances, the Gd- O_2 becoming the shortest. In contrast to the O_1 oxygen the O_2 ions do not mediate any magnetic frustration and thus at $T > 12$ K, the frustration weakens and thus the extra polar displacements.

In conclusion, we report the first powder neutron diffraction on an isotope enriched compound of GdMn_2O_5 . The refined magnetic structure in the commensurate and ferroelectric phase shows a comparable magnetic structure to most of the others members of the RMn_2O_5 series: spins in the (a, b) plane. In the context of the Exchange Striction mechanism, we show in this paper that not only the release of the frustration related to the $\text{Mn}^{3+}\text{-Mn}^{4+}$ J_3 interaction is at play, but an additional exchange-striction effect, releasing the J_6 frustration between the huge and isotropic Gd^{3+} moments and the Mn^{3+} spins, is responsible for a large extra term in the polarization. These findings suggest that the isotropic character and thus the spin-orbit coupling may play a crucial role in the polarization amplitude yet to be confirmed. As a conclusion, one may foresee that the complete and accurate understanding of the role of the rare earth in the multiferroic properties of this series of compounds paves the way to exploratory research on spin-induced multiferroic materials where the choice of rare earth will be a tool to improve the performances.

This work was supported by project CMCU PHC UTIQUÉ 15G1306. The work of M. Greenblatt was supported by NSF-DMR grant 1507252. This work was also supported by Chinese Scholarship Council and NSF-DMR 1507252 grant.

* Present address: Dresden High Magnetic Field Laboratory (HLD-EMFL), Helmholtz-Zentrum Dresden-Rossendorf, 01314 Dresden, Germany.

-
- [1] W. Eerenstein, N. D. Mathur, and J. F. Scott, *Nature* **442**, 759 (2006).
- [2] N. Hur, S. Park, P. Sharma, J. S. Ahn, S. Guha, and S.-W. Cheong, *Nature* **429**, 392 (2004).
- [3] N. Lee, C. Vecchini, Y. J. Choi, L. C. Chapon, A. Bombardi, P. G. Radaelli, and S.-W. Cheong, *Phys. Rev. Lett.* **110**, 137203 (2013).
- [4] A. Inomata and K. Kohn, *J. Phys.: Condens. Matter* **8**, 2673 (1996).
- [5] B. Khannanov, E. I. Golovenchits, and V. A. Sanina, *J. Phys.: Conf. Series* **572**, 012046 (2014).
- [6] D. Lebeugle, D. Colson, A. Forget, and M. Viret, *Appl. Phys. Lett.* **91**, 022907 (2007).
- [7] G. Yahia, F. Damay, S. Chattopadhyay, V. Balédent, W. Peng, E. Elkaim, M. Whitaker, M. Greenblatt, M.-B. Lepetit, and P. Foury-Leylekian, *Phys. Rev. B* **95**, 184112 (2017).
- [8] V. Balédent, S. Chattopadhyay, P. Fertey, M. B. Lepetit, M. Greenblatt, B. Wanklyn, F. O. Saouma, J.I.Jang, and P. Foury-Leylekian, *Phys. Rev. Lett.* **114**, 117601 (2015).
- [9] P. G. Radaelli and L. C. Chapon, *J. Phys.: Condens. Matter* **20**, 434213 (2008).
- [10] S. Petit, V. Balédent, C. Doubrovsky, M. B. Lepetit, M. Greenblatt, B. Wanklyn, and P. Foury-Leylekian, *Phys. Rev. B* **87**, 140301 (2013).
- [11] Y. F. Popov, A. M. Kadomtseva, G. P. Vorob'ev, S. S. Krotov, K. I. Kamilov, and M. M. Lukina, *Phys. Solid State* **45**, 2155 (2003).
- [12] S. Chattopadhyay, S. Petit, E. Ressouche, V. Balédent, S. Raymond, G. Yahia, W. Peng, J. Robert, M. Greenblatt, and P. Foury-Leylekian, accepted in *Scientific Reports* (2017).
- [13] Z. Y. Zhao, M. F. Liu, X. Li, L. Lin, Z. B. Yan, S. Dong, and J. M. Liu, *Scientific Reports* **4**, 3984 (2014).
- [14] M. Tachibana, K. Akiyama, H. Kawaji, and T. Atake, *Phys. Rev. B* **72**, 224425 (2005).
- [15] E. Golovenchits and V. Sanina, *J. Phys.: Condens. Matter* **16**, 4325 (2004).
- [16] C. Doubrovsky, G. André, A. Gukasov, P. Auban-Senzier, C. R. Pasquier, E. Elkaim, M. Li, M. Greenblatt, F. Damay, and P. Foury-Leylekian, *Phys. Rev. B* **86**, 174417 (2012).
- [17] J. Rodriguez-carvajal, *Physica B* **192**, 55 (1993).
- [18] F. Damay, *J. Phys. D: Appl. Phys.* **48**, 504005 (2015).
- [19] L. H. Yin, D. H. Jang, C. B. Park, K. W. Shin, and K. H. Kim, *J. Appl. Phys.* **119**, 104101 (2016), <http://dx.doi.org/10.1063/1.4943587>.
- [20] C. Lu, J. Fan, H. Liu, K. Xia, K. Wang, P. Wang, Q. He, D. Yu, and J.-M. Liu, *Appl. Phys. A* **96**, 991 (2009).
- [21] X. Fabrèges, I. Mirebeau, P. Bonville, S. Petit, G. Lebras-Jasmin, A. Forget, G. André, and S. Pailhès, *Phys. Rev. B* **78**, 214422 (2008).
- [22] I. Lindgren and J. Morrison, *Atomic Many-Body Theory* (Springer-Verlag, 1982).
- [23] N. Suaud and M.-B. Lepetit, *Phys. Rev. B* **62**, 402 (2000).
- [24] A. Gellé and M.-B. Lepetit, *Phys. Rev. B* **74**, 235115 (2006).